Acta Polytechnica CTU Proceedings **33**:212–218, 2022
https://doi.org/10.14311/APP.2022.33.0212

TENSILE BEHAVIOR OF NEWLY DEVELOPED UNDERCUT ANCHOR IN CRACKED AND UNCRACKED CONCRETE

Tomoyuki Hatanaka[a,*], Naoki Funaki[b], Reiji Tanaka[b], Shogo Fujita[c]

[a] *National Institute of Technology, Yonago College, 4448 Hikona-cho, Yonago, Tottori, 683-8502, Japan*
[b] *Tohoku Institute of Technology, 35-1 Yagiyama Kasumi-cho, Taihaku-ku, Sendai, 982-8577, Japan*
[c] *FS Technical Co., Ltd., 1-22-15 Takasa, Katsushika-ku, Tokyo, 125-0054, Japan*
[*] corresponding author: hatanaka@yonago-k.ac.jp

Abstract.
The authors have been designing a post-installed anchor that fixes itself into concrete material by expanding the anchor tip in an upward direction, and conducted tensile loading tests to confirm its fundamental dynamic characteristics. The test results on three types of test specimens, with anchor morphology as a parameter, indicate that the final failure modes were all anchor bar fractures, and a stable yield strength was confirmed. Additionally, the yield strength characteristics of the proposed anchor in cases where cracks are present on the concrete surface, wherein the anchors are fixed, were experimentally confirmed.

Keywords: FEM Analysis, hybrid post-installed anchor, self-detecting damaged state function, tensile load test.

1. Introduction

The concept of "building longevity" plays an important role in the reduction of global greenhouse gas emissions with regards to global environmental problems. There are two primary factors that determine the lifespan of buildings: one is the decline of aseismic performance over time, and the second is the obsolescence of buildings as the functional demands imposed on them change with time. Solutions to these factors include seismic repairs and renovations. Various post-installed anchors are used when installing aseismic materials and equipment in existing buildings, and it is predicted that future use of post-installed anchors will continue to increase to achieve longer lifespans for buildings. Meanwhile, accidents have occurred owing to the age-related degradation of anchors and cracks in the concrete skeleton structure; hence, an anchor that exhibits stable performance even under harsh conditions is necessary for the wide-range and long-term usage of anchors.

With this in mind, the authors have designed multiple types of undercut post-installed anchors with different morphologies. A previous report confirmed the basic dynamic characteristics of the anchors and their performance superiority based on loading test results conducted with these anchors as the test specimens [1–5].

The objectives of the present report are to show the tensile loading test results obtained on post-installed anchors designed by the authors where the anchor tip expands in an upward direction, and to confirm the fundamental yield strength characteristics of the proposed anchor based on these results.

2. Experimental investigation

2.1. Test specimen

Details of the anchor investigated in the present report are shown in Figure 1 and Table 1, and a complete view of the anchor is shown in Figure 2. The proposed anchor is composed of a main body, an expanding cap, and an anchor bar. As shown in Figure 3, the anchor is placed in a hole with an expanded base. The expanding cap, which is fixed at the anchor bar tip, has four slits; by driving the main body into it, the wedge-shaped tip of the main body cuts into the expanding cap, forcing it to expand radially upwards and fix itself into the concrete slab.

The hole into which the anchor is inserted is created by first making a hole using a hammer drill with a straight-drill attachment, and then expanding its base using a specialized hole drill with an expanding bit.

In total, three types of anchors with different anchor bar diameters were chosen as the test specimens, and loading tests were conducted on five samples of each type. The concrete slab into which the anchor is applied is a reinforced concrete plate with dimensions of 1,200 mm × 1,800 mm × 400 mm (length × width × thickness), and reinforced steel (D13) was applied in a grid-like manner to prevent fracture formation on the bottom face. The target compression strength of the concrete slab was set as a constant, with a value of 18 N/mm^2. The actual measured compression strength of the concrete prior to the loading tests was 19.0 N/mm^2. A total of $10-12$ anchors were applied for a single concrete specimen. SUS316 was used as the material for the main body and expanding cap of the anchor, and SUS316L was used

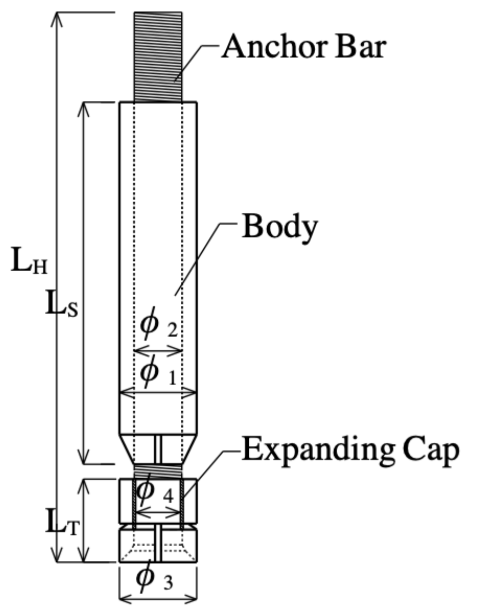

Figure 1. Detail of the anchor specimen.

Figure 2. View of the anchor specimen.

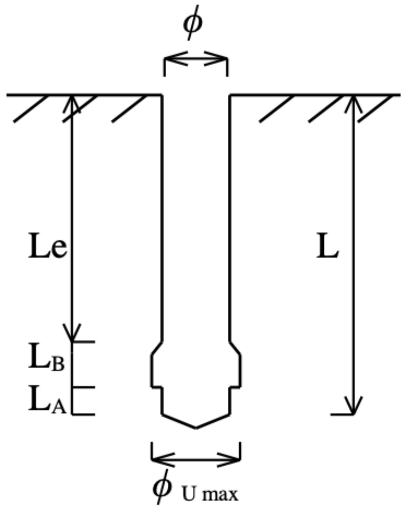

Figure 3. Detail of borehole.

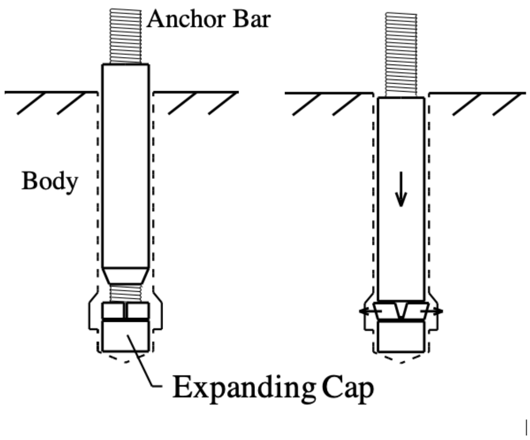

Figure 4. Scheme of the anchor.

for anchor bar.

2.2. Test specimen

The detail of the test setup used for the loading tests is shown in Figure 5, and an overall view of the test setup is shown in Figure 6. The loading tests were conducted using an electrically powered hydraulic jack with a maximum capacity of 400kN, where tensile forces were applied to the anchor bar.

The tensile load was measured by a center-hole-type load cell with a maximum capacity of 200 kN. Additionally, a displacement-measuring plate was attached to the anchor bar, as shown in Figure 5, to measure anchor displacement. The position of the plate attachment was set at approximately 10 mm from the test specimen surface to minimize the effects of elongation on the anchor bar caused by loading. Anchor displacement was measured using three displacement transducers attached between the plate and the displacement-measuring jig set up on top of the test specimen. The displacement shown in this report is the average of the values measured by these three displacement transducers.

2.3. Test results

A representative load-displacement curve obtained by conducting the loading tests are shown in Figures 7 (a) - 9 (a), and the appearance of the anchor after testing are shown in Figures 7 (b) - 9 (b). Additionally, an overview of the test results are shown in Table 2.

These results show that the maximum load increases with increased anchor bar diameter and that the failure mode for all test specimens is the anchor bar fracture. Additionally, differences in the coef-

Configuration	Anchor							Borehole					
	Body			Expanding Cap			Bar						
	L_S	φ_1	φ_2	L_T	φ_3	φ_4	L_H	ϕ	U_{max}	L	L_A	L_B	L_e
M12	104.0	20.5	12.3	22.0	20.0	12.3	180.0	21.0	28.0	132.0	12.0	14.0	106.0
M16	142.0	26.0	16.3	28.0	26.0	16.3	240.0	27.0	36.0	176.0	15.0	19.0	142.0
M20	177.0	32.0	20.3	38.0	32.0	20.2	300.0	33.0	44.0	220.0	18.0	25.0	175.0

Table 1. Main parameters of the anchor specimen and borehole.

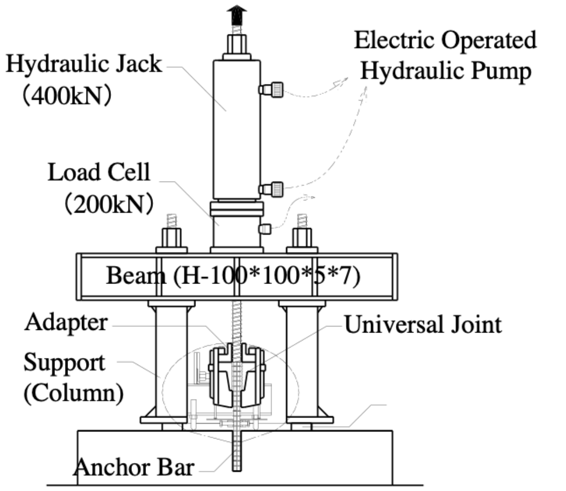

Figure 5. Test setup.

ficient of variation for the maximum yield strength between the anchor bar diameters were small, and a stable tensile yield strength was observed in all the test specimens. As shown in Figures 7 (b) - 9 (b), there were virtually no cases where the main body of the anchor slipped out of its hole due to loading.

Figure 6. Overall view of test set.up.

3. Tensile loading tests in cracked concrete

3.1. Test specimen

Generally speaking, the yield strength of the anchors significantly decreases when cracks are formed on the anchor-applied concrete surface. With this in mind, we created a testing apparatus like the one shown in Figures 10 and 11 to confirm the influence of cracks on the yield strength characteristics of the anchor, and conducted tensile load tests. As shown in the figure, the present testing apparatus is comprised of a pair of guides and moveable blocks into which the concrete block is fixed. The anchors are applied in the upper joined surface sections of the concrete block, and are designed to generate cracks by sliding the moveable block to the left and right. The anchors are connected to air jacks through load cells, and provide strength to the system in the tensile direction. Here, we conducted tests where forces corresponding to the long-term loading in cases where the anchor bar yields were applied at a fixed rate while the crack width of the test specimen was gradually increased. The tensile load was measured using the load cell connected between the jack and the anchor. Additionally, the anchor displacement was measured using the three laser displacement transducers attached to the measuring plate fixed to the anchor bar, and the crack width was measured using six laser displacement transducers set up on the top and either side of the concrete blocks. The anchor displacement and crack width indicated here are the average values between all the measurements made with these displacement transducers. The actual compression strength of the concrete test specimens used in the present test was 19.0 N/mm^2.

3.2. Test results

A representative example of the results obtained from conducting the tests is shown in Figure 12, and the appearance of the anchors after loading is shown in Figure 13. The figure shows the relationship between the extent to which the anchor slipped out, the ap-

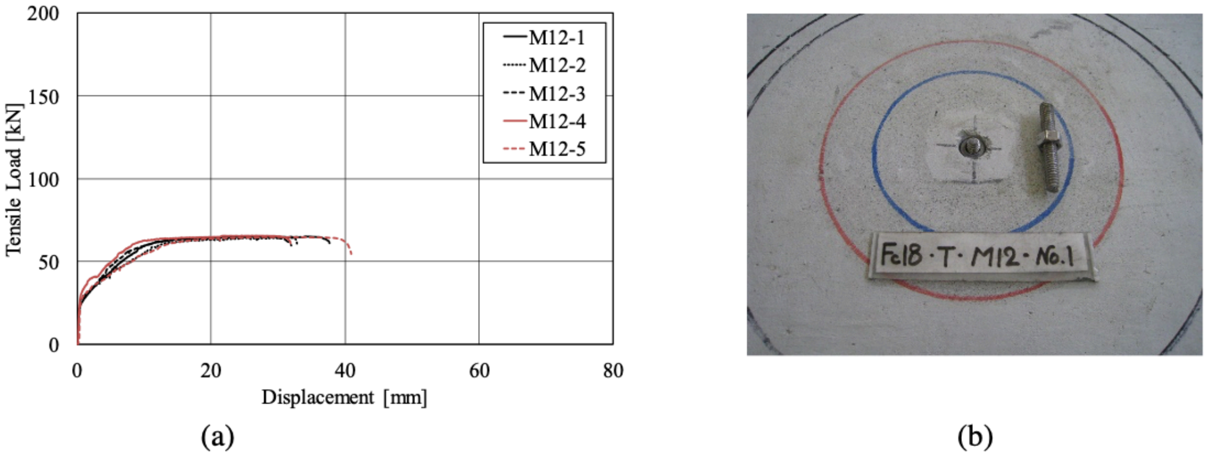

Figure 7. Load-bearing behavior during monotonic tension loading and failure mechanism (M12).

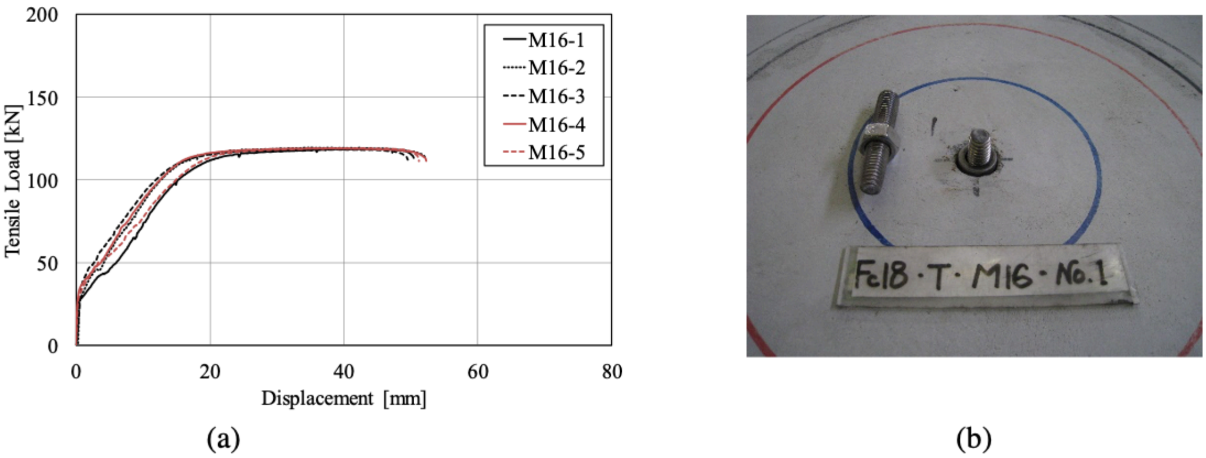

Figure 8. Load-bearing behavior during monotonic tension loading and failure mechanism (M16).

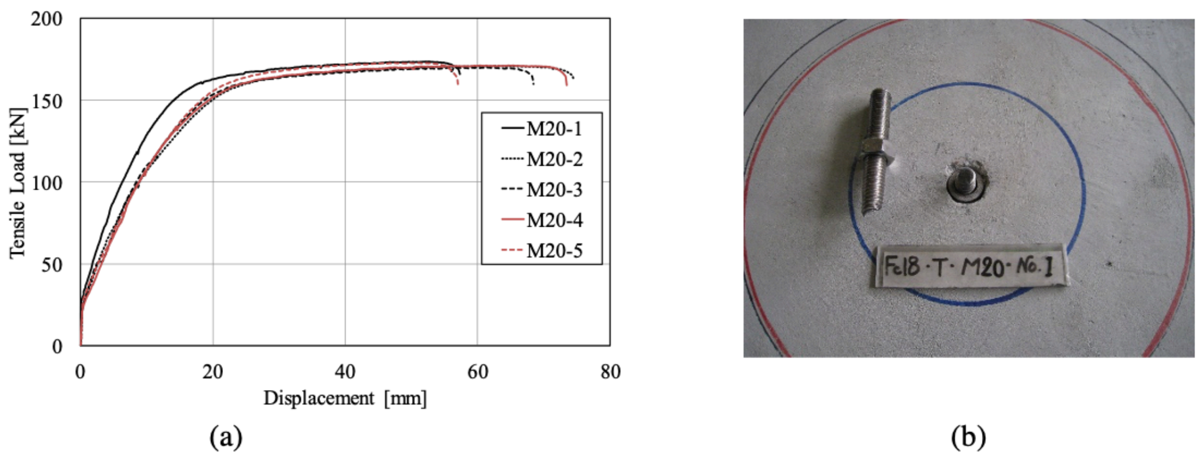

Figure 9. Load-bearing behavior during monotonic tension loading and failure mechanism (M20).

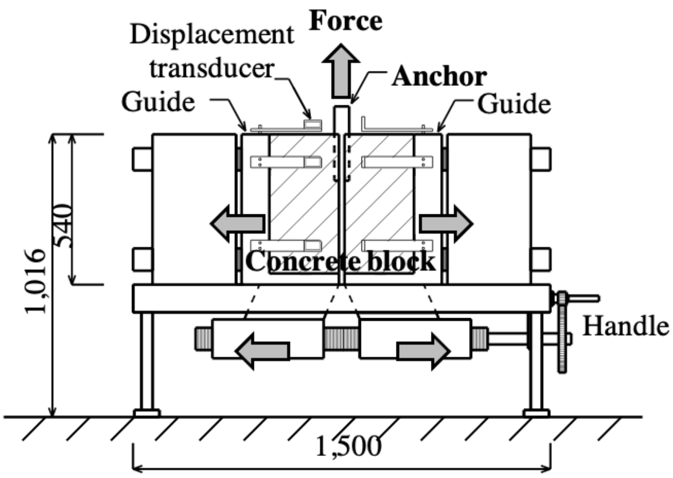

Figure 10. Test setup.

Figure 11. View of test setup.

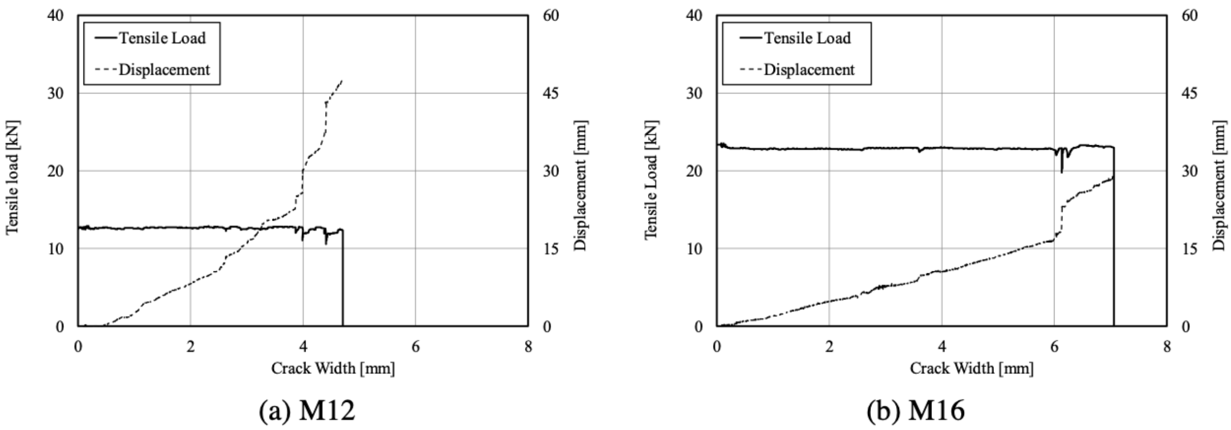

Figure 12. View of test setup.

	Tensile Load [kN]				Displacement [mm]				Failure Type*
	Max.	Ave.	S.D.	C.V.	δ**	Ave.	S.D.	C.V.	
M12-1	65.2				34.1	28.9	3.241	11.2	SF
M12-2	64.5				30.8				SF
M12-3	65.0	65.0	0.323	0.50	27.5				SF
M12-4	65.5				24.6				SF
M12-5	65.0				27.7				SF
M16-1	118.6				42.6	37.4	2.931	7.83	SF
M16-2	119.3				35.0				SF
M16-3	118.4	118.8	0.313	0.26	36.2				SF
M16-4	119.0				34.7				SF
M16-5	118.9				38.6				SF
M20-1	173.6				52.1	55.8	4.270	7.65	SF
M20-2	170.7				60.2				SF
M20-3	169.8	171.7	1.414	0.82	56.6				SF
M20-4	171.4				60.3				SF
M20-5	173.0				49.7				SF

* Max: Maximum Load, Ave: Average, S.D.: Standard Deviation, C.V.: Coefficient Variation [%].
** δ: Displacement in maximum load
*** Max: Maximum Load, Ave: Average, S.D.: Standard Deviation, C.V.: Coefficient Variation [%].

Table 2. Test results***.

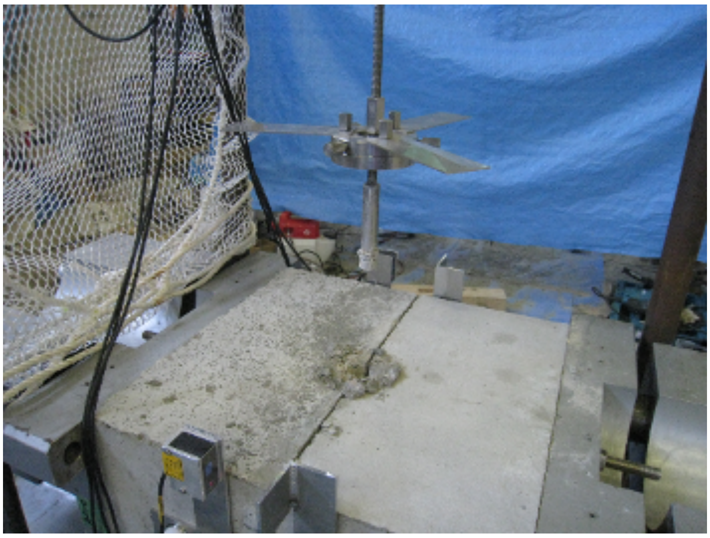

Figure 13. View of test setup.

plied load, and the crack width, obtained by gradually increasing the crack width while applying a load that was equivalent to the long-term loading.

These results showed that the crack width at the time when the main body of the anchor completely slipped out was 4.7mm in the M12 test specimen and 7.1mm in the M16 test specimen, confirming that the yield strength is maintained even in cases where large cracks form on the concrete surface to which the anchors are applied.

4. Conclusion

Tensile load tests were conducted on an undercut post-installed anchor designed by the authors; fundamental yield strength characteristics of this anchor were analyzed based on the obtained results, and the following findings were obtained:

1. The extent of fixation with the concrete base material increased as a result of making the undercut section of the anchor expand in the upward direction, and the anchor exhibited a stable yield strength.
2. The extent of yield strength decreased even in the presence of relatively large cracks. It was lower in the proposed anchor than in standard metal anchors, and its superior performance was confirmed.

Acknowledgements

The authors wish to thank Dr. Akira Shibuya, Technical officials of Tohoku Institute of Technology, for his helpful advice. In addition, kind assistance by Mr. Myunghwan KANG and Tatsuya KUBO, FS Technical Co. Ltd., is deeply appreciated.

References

[1] N. Funaki, A. Shibuya, S. Fujita, et al. Study on the mechanical Properties of expansion post installed anchor, Part 1 Tensile test of expansion post installed anchor equipped with hardware bite. *AIJ summaries of Technical Papers of Annual Meeting*, 377-378, 2017.

[2] M, Onuma, A. Shibuya, N. Funaki, et al. Study on the mechanical Properties of expansion post installed anchor, Part 2 Tensile test of hybrid expansion post installed anchor. *AIJ summaries of Technical Papers of Annual Meeting*, 379-380, 2017.

[3] N. Funaki, A. Shibuya, M. Abe, et al. Study on the mechanical Properties of expansion post installed anchor, Part 3 Shear test of extension post installed anchor equipped with hardware bite. *AIJ Tohoku chapter summaries of Technical Papers of Annual Meeting*, 61-64, 2018.

[4] M. Abe, A. Shibuya, N. Funaki, et al, Study on the mechanical Properties of expansion post installed anchor, Part 4 Mechanical property of L shaped anchor. *AIJ Tohoku chapter summaries of Technical Papers of Annual Meeting*, 65-68, 2018.

[5] T. Hatanaka, N. Funaki, R. Tanaka, et al. Mechanical property evaluation post-installed undercut anchors equipped with hardware bite based on finite element analysis. *JCI Annual Convention*, vol.41, 1279-1284, 2019.